



Published in final edited form as:

Lab Invest. 2012 March ; 92(3): 420–436. doi:10.1038/labinvest.2011.185.

## THE CD133-POSITIVE COLON CANCER CELL PHENOTYPE IS MORE INTERACTIVE WITH THE TUMOR MICROENVIRONMENT COMPARED TO CD133-NEGATIVE CELL

Celia Chao, MD<sup>1,5</sup>, J. Russ Carmical, PhD<sup>2</sup>, Kirk Ives, BA<sup>1</sup>, Thomas G. Wood, PhD<sup>2</sup>, Judith F. Aronson, MD<sup>4</sup>, Guillermo Gomez, MD<sup>1</sup>, Clarisse D. Djukom, MD<sup>1</sup>, and Mark R. Hellmich, PhD<sup>1,3,5</sup>

<sup>1</sup>Department of Surgery, University of Texas Medical Branch; Galveston, TX

<sup>2</sup>Department of Biochemistry and Molecular Biology, University of Texas Medical Branch; Galveston, TX

<sup>3</sup>Department of Neuroscience and Cell Biology, University of Texas Medical Branch; Galveston, TX

<sup>4</sup>Department of Microbiology and Immunology, University of Texas Medical Branch; Galveston, TX

<sup>5</sup>Sealy Center for Cancer Cell Biology, University of Texas Medical Branch; Galveston, TX

### Abstract

Experimental data indicate that colorectal cancer cells with CD133 expression exhibit enhanced tumorigenicity over CD133<sup>-</sup> cells. We hypothesized that CD133<sup>+</sup> cells, compared to CD133<sup>-</sup>, are more tumorigenic because they are more interactive with and responsive to their stromal microenvironment. Freshly dissected and dissociated cells from a primary colon cancer were separated into carcinoma-associated fibroblasts (CAF) and the epithelial cells; the latter were further separated into CD133<sup>+</sup> and <sup>-</sup> cells using FACS. The CD133<sup>+</sup> cells formed large tumors in NOD-SCID mice, demonstrating the phenotypic cellular diversity of the original tumor, whereas CD133<sup>-</sup> cells were unable to sustain significant growth. Affymetrix gene array analyses using t-test, fold-change, and multiple test correction identified candidate genes that were differentially expressed between the CD133<sup>+</sup> vs. <sup>-</sup> cells. RT PCR verified differences in expression for 30 of the 46 genes selected. Genes upregulated (+ vs <sup>-</sup> cells) included CD133 (9.3-fold) and CXCR4 (4-fold), integrin  $\beta 8$  and fibroblast growth factor receptor 2 (FGFR2). The CAF highly express the respective ligands: SDF-1, vitronectin, and FGF family members, suggesting a reciprocal relationship between the CD133<sup>+</sup> and CAF cells. SDF-1 caused an increase in  $[Ca^{2+}]_i$  in cells expressing both CD133 and CXCR4, confirming functional CXCR4. The CD133<sup>+</sup>/CXCR4<sup>+</sup> phenotype is increased to 32% when the cells are grown in suspension, compared to only 9%

Users may view, print, copy, download and text and data-mine the content in such documents, for the purposes of academic research, subject always to the full Conditions of use: [http://www.nature.com/authors/editorial\\_policies/license.html#terms](http://www.nature.com/authors/editorial_policies/license.html#terms)

**To whom correspondence should be addressed:** Celia Chao, MD, Department of Surgery, University of Texas Medical Branch, 301 University Blvd., Galveston, TX, USA 77555-0737, Telephone: (409) 772-0698; Fax: (409) 772-0088; [cechao@utmb.edu](mailto:cechao@utmb.edu).

### CONFLICTS OF INTEREST

The authors declare no conflict of interest.

when the cells were allowed to attach. In Matrigel 3-D culture, the CD133+/CXCR4+ group treated with SDF-1 grew both more colonies compared to vehicle as well as significantly larger colony sizes of tumor spheres. These data demonstrate proof of principle that the enhanced tumorigenic potential of CD133+, compared to CD133-, cells is due to their increased ability to interact with their neighboring CAF.

## Keywords

CD133; colon cancer; CXCR4; tumor microenvironment

Human solid tumors are characterized by phenotypically heterogeneous populations of malignant cells with varying degrees of differentiation and tumor initiating potential. The trans-membrane glycoprotein CD133, originally characterized as a cell surface marker for hematopoietic stem cells (1, 2), identifies a subset of malignant cells with enhanced tumorigenic activity in cancers from a variety of tissues including, prostate, brain, breast, pancreas, liver, uterus and colon (3–12). Similar to the other cancers, CD133-positive (CD133+) cells isolated from colorectal tumors grow in suspension culture as anchorage-independent epithelial spheroids (colospheres) and efficiently initiate new tumor formation when xenografted into immunodeficient NOD-SCID mice (7, 8). Ricci-Vitiani et al. (8) showed that subcutaneous injection of as few as  $3 \times 10^3$  CD133+ human colon cancer cells, suspended in matrigel, generated visible tumors in mice between 4 and 5 weeks post-transplant, whereas injection of as many as  $10^5$  CD133-negative (CD133-) cells isolated from the same patient failed to produce tumors over the same time course. Subpopulations of CD133+ cells isolated from established colon cancer-derived cell lines such as HT29 and LoVo also exhibit increased proliferation, invasion through extracellular matrix (ECM), and colony formation in culture (13), and clinically, the level of CD133 expression in tumor tissue negatively correlates with both disease-free and overall survival of colorectal cancer patients (14–16).

Although the preponderance of data indicates that expression of CD133 identifies a subpopulation of cancer cells with enhanced tumorigenic potential and prognostic value, CD133 does not appear to functionally regulate the aggressive phenotype. This point is illustrated by the observations that siRNA-mediated suppression of CD133 neither compromised the tumorigenic potential of primary human colon cancers cells xenografted in nude mice (17) nor the proliferation, migration, invasion and anchorage-independent growth of CD133+ LoVo and Caco-2 cells in culture (18). Thus a mechanistic explanation for the enhanced tumorigenicity of CD133+ colon cancer cells remains enigmatic.

In addition to cell autonomous properties, the tumorigenicity of cancer cells is also influenced by their interactions with the tumor microenvironment. Solid tumor tissue contains a multitude of non-malignant cells, collectively known as tumor stroma, which directly through cell-to-cell contacts, and indirectly through paracrine signaling networks, mediate regulation of protease activity and modulation of ECM proteins to promote tumorigenesis, angiogenesis and metastatic spread (19, 20). The most prevalent cells found in the tumor stroma are the cancer-associated fibroblasts (CAFs) (21), which in multiple

studies have been shown to promote and/or enhance the tumorigenic potential of both adenoma and adenocarcinoma cells. An example of the former is a study by Olummi et al. (22), in which CAFs isolated from malignant human prostate tissue promoted robust tumor formation when co-injected subcutaneously with an SV40 T-antigen immortalized, but non-tumorigenic, human prostate epithelial cell line called Tag-HPE into immune deficient mice (22), whereas neither the prostate CAFs nor Tag-HPE cell line alone produced tumors when injected into the mice. Similarly, Orimo et al. (23) showed that CAFs isolated from breast cancers, but not normal breast fibroblasts, significantly enhanced the tumorigenicity of human MCF-7-ras breast cancer cells when co-injected into immune-deficient mice, and Hwang et al. (24) demonstrated that tumor-associated human pancreatic stellate cells (an activated myofibroblast-like cell) enhanced the tumorigenicity and metastasis of human BxPC-3 pancreatic cancer cells in mice. Together, these studies demonstrate that CAF can enhance tumor growth and spread. Thus, we hypothesized that the increased tumorigenicity of CD133+ colon cancer cells may be due, in part, to its enhanced interactions with CAFs of the tumor microenvironment.

To begin testing this hypothesis, we performed a comprehensive molecular profiling of CD133+ and CD133- carcinoma cells, as well as of the CAFs isolated from the same patient specimen, in order to reveal phenotypic differences between these cell populations. Herein, we report that, compared to CD133- colon cancer cells, CD133+ cells have reduced transcript levels for cell adhesion and matrix proteins, but increased transcripts for proteases, and cell surface receptors such as the cytokine receptor CXCR4, which mediates tumor cell proliferation and metastasis (25). Additionally, CAFs express the ligands for the receptors overexpressed by the CD133+ cells, including the CXCR4 receptor ligand CXCL12 (also known as stromal derived factor-1 or SDF-1), indicating the potential for enhanced paracrine signaling between these cells. Functional studies confirmed that CD133+ colon cancer cells exhibit enhanced proliferation in response to SDF-1 compared to CD133- cells, supporting the hypothesis that the enhanced tumorigenic potential of CD133+ cells is due, in part, to enhanced paracrine signaling with CAFs of the tumor microenvironment.

## MATERIALS AND METHODS

### Cell isolation and culture

Cell cultures were established from a freshly dissected colon tumor, which was obtained under an IRB-approved protocol from a 68-year-old woman with Stage II (pT3 N0) disease. The tissue was rinsed twice in Dakin's solution (4% boric acid and 0.5% bleach), minced, and digested as described previously (26). Dissociated cells were cultured in DMEM supplemented with 200 U/ml penicillin, 200 µg/ml streptomycin, 0.25 µg/ml amphotericin B, and 50 µg/ml gentamicin (Invitrogen, Carlsbad, CA), 10% fetal bovine serum, and 1% insulin-transferrin-selenium (ITS) (Invitrogen, Carlsbad, CA). Using a tumor outgrowth procedure, we isolated and separately cultured both the carcinoma cells and CAF from the same tumor. Suspension epithelial cell cultures were grown in ultra-low adhesion flasks (Costar; Corning; Lowell, MA). The isolated CAF were grown in standard tissue culture flasks (Cellstar; Grenier Bio-One; Monroe, NC). Both the carcinoma cells and CAF were

maintained in the DMEM, 10% FCS, 1% ITS, 1% nonessential amino acids (Invitrogen), and 1% penicillin-streptomycin.

### **Immunocytochemistry (ICC)**

Verification of epithelial and mesenchymal cell types was performed by ICC as described previously (26). Briefly, cells were fixed in 4% paraformaldehyde, rinsed with PBS and then permeabilized in absolute methanol (ice-cold) for 10 min. The coverslips were then placed in 2% milk for blocking and then rinsed in PBS 1% BSA. Primary antibody incubation for 1 h R.T, rinsed, and then secondary antibody applied for 1 h RT. Antibodies used were pan-cytokeratin AE1/3 (1:200 dilution; Santa Cruz),  $\alpha$ -SMA (Sigma A5228; 1:200), and vimentin (Sigma V6630; 1:40). Secondary antibodies (1:200) used were either goat anti-rabbit IgG or goat anti-mouse IgG labeled with Alexa 546 and 488 (Molecular Probes; Eugene, OR), respectively.

### **Immunohistochemistry (IHC)**

Spheroids were fixed in 10% neutral formalin for 24 h, immobilized in 2% agar solution, and embedded in paraffin blocks and sectioned (5  $\mu$ m). Prior to staining, the sections were deparaffinized with xylene, dehydrated with ethanol, and subjected to antigen retrieval using citrate buffer (10 nM pH6 at 98C for 20 min) to optimize antigen immunoreactivity. Antibodies for IHC included CD133 (AC133/1, 1:50 dilution, Miltenyi Biotec), CD44 (1:50, Cell Signaling), MUC4 (Clone 1G8, 1:100; Invitrogen), CEA (1:800; Biocare Medical; Concord, CA), CD34 (1:100; Biocare), CD166 (1:400, GeneTex; Irvine, CA),  $\alpha$ SMA (ab5694, Abcam, 1:400), and Mayer's mucicarmine (Poly Scientific; Bay Shore, NY). Additionally, CK7 (1:200), CK20 (1:100), Ki67 (1:100), and the universal negative control for anti-rabbit and anti-mouse IgG were all purchased from Dako (Carpinteria, CA). The ApopTag® Peroxidase in Situ Apoptosis Detection Kit was used to detect apoptotic cells by labeling and detecting DNA strand breaks by the TUNEL method (Millipore; Billerica, MA). The streptavidin biotin technique was used to visualize the immunostain. The slides in Figures 8 and 9 underwent a tertiary step with streptavidin alkaline phosphatase at 1:200 for 15 min (Vector Labs, SA-5100) and the chromagen was fast red for 5 min.

### **Cell sorting**

Cells were dissociated in Accumax (Innovative Cell Technologies, Inc., San Diego, CA) and resuspended in PBS containing 0.5% BSA and 2 mM EDTA. Human FcR blocking reagent was used to block non-specific Fc receptor-mediated antibody labeling. FACS with a FACSAria (Becton Dickinson Biosciences, San Jose, CA) s. analysis was performed using monoclonal antibodies for CXCR4 (clone 12G5; BD Biosciences), CD133/1 (AC133) conjugated to R-phycoerythrin (PE) or allophycocyanin (APC), and isotype-matched IgG controls (Miltenyi Biotec; Auburn, CA).

### ***In vivo* tumorigenicity assay**

CD133+ and – cells were purified by FACS sorting. Serial limiting dilution of equivalent numbers of both CD133+ and – cells mixed 1:1 in growth factor reduced Matrigel (BD Biosciences, San Jose, CA) and phosphate buffered saline (PBS) were injected

subcutaneously into a 10-week-old male non-obese diabetic- severe combined immunodeficient (NOD-SCID) mice under an IACUC-approved protocol. Tumor sizes were measured transcutaneously over time. Tumor weight and tumor volumes [ $V=(\pi/6)hd^2$ ] were obtained at 6 weeks. Specimens were fixed with 10% formalin and embedded in paraffin. Sections were stained with hematoxylin and eosin (H&E).

### Gene Expression Analysis

Total cellular RNA was extracted using RNAqueous (Ambion; Austin, TX) according to the manufacturer's recommendations from three pairs of samples (CD133+ and CD133-) that were sorted on three separate days. Total RNA was also prepared from three separate CAF cultures in the same manner. RNA was quantitated using a NanoDrop ND-1000 (NanoDrop Technologies, DE, USA). RNA integrity was assessed by visualization of 18S and 28S RNA bands using an Agilent BioAnalyzer 2100 (Agilent Technologies, CA). Total RNA extracted from the samples was processed using the RNA labeling protocol described by Ambion (MessageAmp™ aRNA Kit Instruction Manual) and hybridized to Affymetrix Gene Chips™ (HG133 Plus 2.0 arrays). Data quality was assessed by applying the quality matrix generated by Affymetrix GeneChip™ Command Console (AGCC) software. The resulting data was analyzed with Partek Genomics Suite (Partek Incorporated, MO, USA). Principal component analysis as a quality assurance measure was performed. The raw data was normalized through robust multichip averaging upon import to Partek Genomics Suite. To identify differentially expressed genes, an ANOVA was applied to the extracted gene expression measures. In order to reduce the occurrence of false positives multiple test corrections (Benjamani-Hochberg and Bonferroni) were applied. The data set was filtered for a p-value of < 0.05 and <0.01 resulting in the final list of differentially expressed genes.

### Real-time quantitative polymerase chain reaction

Real Time SYBR® Arrays were utilized to validate a subset of the genes generated by the analysis of the Affymetrix gene expression data. This approach combines the quantitative performance of SYBR® Green-based real-time quantitative PCR with the multiple gene profiling capabilities of a microarray. The real time array is a 96-well plate containing qPCR primer assays for 45 genes of interest plus 3 housekeeping genes (GAPDH, Rpl19 and Bpol) to serve as normalizers. The 48 assays were duplicated on same the plate to facilitate comparison of CD133+ & CD133- samples and eliminate plate to plate variance. Biological replicate sets (test, control) were assayed on three separate plates for proper statistical analysis. A melt curve was carried out at the end of each PCR run protocol to identify multiple PCR products that would confound the data. The list of primers used is shown in Table 2 of Supplemental Materials.

Total RNA (1 ug) was used in the Affymetrix gene expression analysis was used in a single reverse transcription reaction to generate cDNA. The resulting product was distributed equally among the 48 wells containing the assay primers. The assays were carried out under standard real time run parameters specific to the Taq polymerase (Applied Biosystems, Foster City, CA) being used. Delta CT values were calculated and used to determine fold changes. Student's t-test was carried out on the biological replicates in order to determine the degree of confidence at which differential expression can be discerned.

### Intracellular calcium imaging

Single cell recordings of agonist-mediated increases in intracellular calcium ( $[Ca^{2+}]_i$ ) was performed as described previously (27). Briefly, cells were washed in KRH physiological medium and then loaded with 2.5  $\mu$ M of the calcium sensing dye Fura-2 AM ester (Molecular Probes; Eugene, OR) with 0.055 Pluronic F-127 (wt/vol) for 50 min at 25°C. Changes in  $[Ca^{2+}]_i$  were monitored with a Nikon Diaphot inverted microscope (Nikon Instrument Group, Garden City, NY) equipped with a Nikon 40X (1.3NA) Neofluor objective. The fluorescent light source was a PTI deltaScan RD-1 ratio fluorescence spectrometer system, equipped with a light-path chopper and dual-excitation monochrometers. The Fura-2 was alternately excited at 340 and 380 nm, and fluorescence emission was monitored through a 510 nm bandpass filter (Omega) with a Photometrics Coolsnap EZ camera (Tucson, AZ). Increases in  $[Ca^{2+}]_i$  were recorded in response to 400 ng/ml of the ligand stromal-derived growth factor-1 $\alpha$  (SDF-1 $\alpha$ ) (Peprotech; Rocky Hill, NJ) at room temperature to verify the presence of functional CXCR4.

### Matrigel culture

Cells were embedded in Matrigel (BD Biosciences; San Jose, CA) in the top of a transwell insert (8  $\mu$ m pore, Costar) in duplicate. A single treatment of SDF-1 $\alpha$  (400 ng/ml) or vehicle (0.2% BSA) was placed in the bottom well in DMEM. Cells were allowed to grow. After 30 days, the number of cell clusters was quantified by visual counting using a 25 mm<sup>2</sup> reticle (Upstate Technical Equipment Company, Inc., East Syracuse, NY). The size of the cell clusters were measured with a micrometer. Student's t-test was used to assess significance between the paired groups, defined at  $p < 0.05$ .

## RESULTS

### Isolation and characterization of human colon cancer cells and CAFs

Colon cancer cells and CAFs were isolated from a freshly resected Stage II, moderately differentiated, right colon tumor in accordance with an institutional-approved IRB protocol as described in Methods. The primary cell culture, named CT03, consisted of two morphologically distinct cell populations: non-adherent clusters of cells and adherent cells that spread on the bottom of the tissue culture flask, (Fig 1A). Immunocytochemical analysis identified the spheroid-cell clusters (colospheres) as cytokeratin-positive (Fig 1B), CD34-negative (data not shown) cells, whereas, the adherent cells stained positive for vimentin and but were negative for cytokeratin expression (Fig 1C), consistent with a fibroblast phenotype. A subpopulation of the vimentin-positive adherent cells also expressed  $\alpha$ -smooth muscle actin (SMA) (Fig 1C), suggestive of myofibroblasts (28).

### Isolated colospheres exhibit phenotypic heterogeneity and are similar to the surgical specimen

Cells within the colon epithelial spheroids exhibit phenotypic heterogeneity and varying degrees of differentiation. Similar to the patient's original tumor (Fig 2), a subpopulation of cells express CD133. Glycosylated CD133 localizes to the apical microvilli of primitive epithelial cells (29) and on the luminal surface of the glands (15); this pattern of expression

is recapitulated in the colon spheroids (Fig 2). Cross-sections of the colospheres demonstrate that the central core do not express CD33, but are apoptotic, as evidenced by the stain for TdT-mediated dUTP Nick-End Labeling (TUNEL). Cells peripheral to the core, however, are highly proliferative, with  $59.9 \pm 8.8\%$  (mean  $\pm$  SEM) of the cells showing strong immunostaining for nuclear Ki67. Some cells within the spheroids exhibited glandular organization, with positive mucicarmine staining within acellular lumens (Fig 2, pink areas indicate presence of mucin). The original tumor stained positive for mucicarmine and also a specific mucin protein, MUC4. Both the patient tumor and the colospheres stained positive for the cell-surface glycoprotein carcinoembryonic antigen (CEA) (Fig 2). Although prior reports indicate that CD133+ colon cancers do not express CK20 (13, 30), the spheroid cells did rarely express CK20, consistent with the original tumor which was predominately negative for CK20, with only a small proportion of the tumor sampled positive for CK20. CK20 is a marker for the differentiated phenotype of colorectal cancers, expressed in up to 92% of colon cancers (31). CK7-positive tumors characterizes only 16% of all colorectal cancers, while colorectal cancers that express both CK20 and CK7, such as this patient's tumor represent only 12% (31). This phenotype is recapitulated in the cultured colospheres (Fig 2). Finally, most cells within the spheroids as well as the original tumor sample express both CD44 and CD166, both putative colon cancer stem cell surface protein markers (32, 33).

### **CD133+ cells exhibit enhanced tumorigenicity when compared to CD133- cells**

To assess the relative tumorigenicity of the subpopulation CD133+ cells, the epithelial spheroids were dissociated into single cells using Accumax (Innovative Cell Technologies; San Diego, CA), labeled with fluorescently-tagged antibody to CD133 (AC133), and separated by fluorescence-activated cell sorting (FACS) (Fig 3A). Cells exhibiting the highest level of CD133 expression (CD133+ cells) were separated from the cells expressing very low levels detectable CD133 (Fig 3B, similar expression levels as cells labeled with non-specific IgG control antibody). To evaluate tumorigenicity, the sorted cells were serially diluted and resuspended in growth factor-reduced Matrigel. CD133+ cells transplanted subcutaneously at  $10^3$  were able to form tumors in NOD-SCID mice, whereas CD133- cells were either unable to sustain growth or formed very small tumor masses (Fig 3C and D). Tumor volumes at 6 weeks were  $11 \pm 4$  and  $420 \pm 114$  mm<sup>3</sup> (CD133- vs. CD133+, respectively,  $p=0.01$ , t-test) (Fig 3D). The tumors harvested from the xenograft demonstrate phenotypic cellular heterogeneity similar to the primary tumor tissue isolated from the patient (Fig 3E and H, respectively). Regions of the xenograft tumor displayed both moderately-differentiated (Fig 3F) and well-differentiated cancer (Fig 3G), recapitulating the histopathology of the patient's tumor (Fig 3I and J, respectively).

### **Gene Expression Analysis: Comparison of CD133+, CD133-, and CAF cells**

**Overview**—In order to explain the different *in vivo* biologic behaviors, we hypothesized that the increased tumorigenicity of CD133+ colon cancer cells may be due, in part, to enhanced interactions with CAFs of the tumor microenvironment. Using the Affymetrix Gene Chip platform (HG133 Plus 2.0 array), we 1) compared the differential gene expression between CD133+ and CD133- cells, and 2) examined the reciprocal receptor-ligand relationships between the epithelial cells (CD133+ or CD133-) and CAF isolated

from the same tumor. As expected, unsupervised hierarchical clustering showed that the CAF and the epithelial cells clustered at opposite ends of the dendrogram, confirming that CD133+ cells were more similar to CD133- cells, than they were to the CAF (Fig 4).

ANOVA analysis of the CD133+ versus CD133- carcinoma cells revealed 1410 and 318 differentially expressed genes significant at the p 0.05 and 0.01 level, respectively. To reduce the false discovery rate, two multiple test corrections were applied to the 1410 genes list: The method of Benjamani and Hochberg identified 1155 gene transcripts, whereas the very stringent Bonferroni correction only identified 35 significant genes. We selected 45 of the 1155 genes for real-time PCR validation (qPCR). Of the 45 genes selected, all 14 of gene transcripts evaluated as significant by Bonferroni correction, were also verified by qPCR (data not shown). However, many true positive results would have been excluded with this level of stringency. Of the 45 genes selected that were significant by the Benjamani-Hochberg analysis ( $p < 0.05$ ), 27 of 45 genes (60%) were concordant by qPCR (Table 1).

**Similarities between CD133+ and CD133- cells**—Because this isogenic cancer cell line was segregated by CD133 expression levels, as expected, gene array results verified that PROM1 (CD133) was 9.3-fold enriched in the CD133+ cells compared with the CD133- cells (Table 1). Many investigators have suggested that other stem cell markers such as CD44 (a subset of CD133+ cells), EpCAM, and CD166 (30, 32) select for *in vivo* tumorigenesis in immunodeficient mice. In our microarray analysis, there were no appreciable differences in the co-expression of other putative colon cancer stem cell markers CD44, EpCAM, Lgr5, CD166, CD49b, Bmi1, between the CD133+ and CD133- cells (Supplemental Table 1). To determine whether key genetic determinants of the adenoma-to-carcinoma sequence are differentially expressed by CD133+ versus CD133- colon cancer cells, we compared the gene expression levels of oncogenes (Src, Raf-1, Met, K-ras), tumor suppressor genes (APC, DCC, TP53, PTEN), DNA mismatch repair genes (MLH1, MSH2, MSH, MGMT) and other genes specific for colon carcinogenesis (CHK2, TGFBR2). No statistically significant differences were identified between CD133+ and - cells, indicating that the cells share the same genetic background for colon cancer-specific oncogenes and tumor suppressor genes (Supplemental Table 1).

**Differences between CD133+ and CD133- cells:** Our analysis revealed gene expression differences between CD133+ and CD133- cells in three major categories: cell adhesion/matrix proteins, matrix-digesting proteases, and cell surface receptors involved in proliferation/metastasis (Full gene list available at GEOarchive at [www.ncbi.nlm.nih.gov/geo](http://www.ncbi.nlm.nih.gov/geo)). Specifically, genes downregulated in CD133+ relative to CD133-cells included the extracellular matrix proteins: COL1A1 (collagen type1 $\alpha$ 1; -3-fold), COL1A2 (collagen 1 $\alpha$ 2; -5-fold), fibronectin (FN1; -3.8-fold), chondroitin sulfate proteoglycan 2 (CSPG2; -2.5-fold), and osteonectin (SPARC; -7-fold). CD133+ also exhibited increased expression, relative to CD133- cells, of proteases that may mediate degradation of extracellular matrix proteins and facilitate cell migration including: cathepsin C (CTSS; 1.65-fold), transmembrane protease-serine 3 (TMPRSS3; 2.15-fold) and sulfatase-2 (SULF2; 2.21-fold). CD133+ cells, compared to CD133- cells (Table 2A), overexpressed transcripts for



cell surface receptors that may mediate cell surface-linked inter-cellular signal transduction, such as CXCR4 (4-fold), a chemokine receptor vital to stem cell growth and homing, integrin  $\beta$ 8 (ITGB8, 2.1-fold-increase), CD74 molecule (CD74; 3.1-fold), and fibroblast growth factor receptor-2 (FGFR2, 1.2-fold). The transcripts for the cognate ligands CXCL12 (also known as stromal-derived growth factor, SDF-1, the ligand for CXCR4), macrophage inhibitory factor (MIF, the ligand for CD74), vitronectin (VTN, a ligand for ITGB8), and fibroblast growth factor family members (FGF, ligands for FGFR2), are all expressed equally by both CD133+ and CD133- cells (Table 2A). Compared to the CD133+ or CD133- carcinoma cells, the CAF cells, isolated from the original patient cancer specimen, demonstrate high expression levels for CXCL12, MIF, VTN or the FGF ligands (Table 2B). However, only the CD133+ cells significantly overexpressed the corresponding cell surface receptors for the ligands: CXCR4, CD74, ITGB8, FGFR2 (Table 2C), indicating that only the CD133+ cells, but not CD133- cells, have a strong reciprocal relationship with the CAF. Together, these results are consistent with the hypothesis that the CD133+ cells may be better positioned to engage in paracrine signaling with CAF in the microenvironment.

### **The CD133+/CXCR4+ phenotype can be maintained in anchorage-independent culture conditions**

To test if cells that are enriched for CD133+ can propagate and maintain CD133+/CXCR4+ cell surface expression in culture, we sorted the colospheres into CD133+ and CD133- single cells and maintained each cell population in low-adhesion flasks. After 9 weeks, repeat FACS analysis demonstrated that the CD133+ group continued to remain relatively enriched for CD133 cell surface expression (Fig 5A), with a proportion of CD133+ cells also co-expressing CXCR4 (Fig 5B). The CD133- group maintained minimal CD133 and CXCR4 expression, (Fig 5A and B).

To evaluate whether cell culture conditions affected CD133/CXCR4 expression, the cells were grown either in a suspension culture using low-adhesion flasks or allowed to adhere onto tissue-culture plastic. If the cells were grown in low adhesion flasks, the cells grew in suspension as spheres, as expected (Fig 6A). However, if the cells were grown in standard tissue culture plastic, after approximately 2 weeks, most of the cells settled to the bottom of the flask and grow as a monolayer in an anchorage-dependent manner (Fig 6B). If the colon cancer cells were allowed to grow as a suspension culture, there was marked enrichment of the double-positive (CD133+/CXCR4+) phenotype (32% of the total cell population), compared with the same cells grown as a monolayer (9% of the total cell population) (Fig 6C and D, respectively). Conversely, the CD133-/CXCR4- phenotype was increased to 46.7% of the total monolayer cell population if grown in adherent flasks compared to 29.8% if grown in suspension. Therefore, these results indicate that the anchorage-independent growth condition (suspension culture) preferentially enriched for the CD133+/CXCR4+ cell type, whereas the anchorage-dependent growth condition selected for the CD133-/CXCR4- phenotype.

### **CD133+/CXCR4+ cells have functional CXCR4**

Since the gene array analysis revealed that CXCR4 was over-expressed 4-fold in the CD133+ over the CD133- cells, we validated functional CXCR4 in CD133+ cells using

two-color FACS and selecting for the relative presence or absence of CD133, as well as the relative presence or absence of CXCR4. CXCR4 is a G-protein coupled receptor activated by the chemokine SDF-1 $\alpha$ , initiating a signal transduction cascade involving the generation of inositol triphosphate, release of intracellular calcium, and activation of downstream kinases that affect cellular proliferation, migration, and invasion (23, 34, 35). An increase in intracellular calcium was measured in 75% of the double positive (CD133+/CXCR4+) cells in response to ligand SDF-1 $\alpha$  (400 ng/ml) (Fig 7A), confirming the presence of functional receptor. We used carbachol (10  $\mu$ M) as a positive control to assure that the cells were adequately loaded with the calcium indicator dye Fura-2. The M<sub>3</sub> muscarinic receptor has been shown to be expressed in most human normal and colon cancer tissue tested (36), and thus, the acetylcholine agonist carbachol should elicit an increase in intracellular calcium on the cells (Fig 7A–C). As expected, SDF-1 $\alpha$  did not stimulate a calcium response in the CD133+/CXCR4–, nor the CD133–/CXCR4– cell fractions (Fig 7B and C, respectively), demonstrating the lack of functional CXCR4 in these cell subpopulations. This assay was not performed on the CD133–/CXCR4+ cells because this fraction represented a small minority (<10% total cell population) and the amount of healthy live cells retrievable for this assay was insufficient for analysis.

### **SDF-1 $\alpha$ stimulates growth in CD133+/CXCR4+ cells**

CAF-derived SDF-1 $\alpha$  has been shown to stimulate carcinoma cell growth directly through the CXCR4 receptor on the cancer cell (23). Coculture of CAF with the epithelial cells will not directly test whether SDF-1 $\alpha$  can stimulate CD133+/CXCR4+ cell growth because CAF secrete multiple growth factors, which may stimulate other CD133+ cell surface receptors. To eliminate potential confounding conditions, we performed *in vitro* growth assays by adding SDF-1 $\alpha$  directly to the colospheres embedded in Matrigel. Cells were sorted with dual color FACS for CD133 and CXCR4 and allowed to grow either in the presence of SDF-1 $\alpha$  (400 ng/ml) or vehicle (0.2% BSA). After 30 days, both the total number of cell colonies and the mean diameter of each colony were assessed. The CD133+/CXCR4+ group treated with SDF-1 $\alpha$  sustained the growth of more colonies compared to vehicle (80 $\pm$ 1.5 vs. 67 $\pm$ 3.5, respectively, Figure 7D), as well as significantly larger colony sizes of tumor spheres (25 $\pm$ 0.01 vs 17 $\pm$ 0.008  $\mu$ m diameter, Student's t-test, p<.0002) (Fig 7G). The CD133+/CXCR4– (Figure 7E) cells formed fewer tumor colonies (68 $\pm$ 2 colonies in the presence of SDF-1 vs. 62 $\pm$ 4 colonies with vehicle) compared to the double-positive cells. However, unexpectedly, the CD133+/CXCR4– cells treated with SDF-1 $\alpha$  grew larger colonies compared to the same cells treated with vehicle (21 $\pm$ 0.009 and 16 $\pm$ 0.006  $\mu$ m, respectively, t-test, p<0.0001, Fig 7G). This result may be explained by the fact that the sorted CXCR4-negative cell fraction express relatively less CXCR4 compared to the CXCR4+ fraction, but is not completely depleted of all CXCR4-positive cells. Finally, cell colonies characterized by CD133–/CXCR4– (Fig 7F) formed only 48 $\pm$ 3 and 26 $\pm$ 9.5 colonies in the presence of ligand and vehicle, respectively, with average size per colony of 16 $\pm$ 0.005 vs. 14 $\pm$ 0.01  $\mu$ m. CD133–/CXCR4+ cells were relatively rare and those that were retrieved after cell sorting did not survive in culture. In summary, cells co-expressing both CD133 and CXCR4, when treated with SDF-1 $\alpha$ , sustained the greatest number of spheroid colonies and the largest diameter per colony of spheroid colonies.

## CD133+ cells are spatially located adjacent to a relative abundance of CAF in colorectal cancer

To show that CD133+ cells are spatially in close proximity to CAF in the original tumor sample, we co-stained a formalin fixed paraffin-embedded block for CD133 (shown in red) and  $\alpha$ -SMA (brown) (Fig 8). CD133- cells are not surrounded by  $\alpha$ -SMA-positive CAF (Fig 8A), whereas, in contrast, the CD133+ cells are surrounded by CAF (Fig 8B). Using tumor samples from another 11 CD133+ colon cancer specimens, we demonstrate that CD133+ cells have a greater propensity to be situated adjacent to CAF ( $\alpha$ -SMA-positive cells), compared to CD133- cells (Fig 9). Under an IRB-approved protocol, we performed dual staining of CD133 and  $\alpha$ -SMA. Fig 8C demonstrates in another patient that the normal margin colonic villi are surrounded by some  $\alpha$ -SMA-positive fibroblasts. The carcinoma from the same patient (as Fig 8C) is characterized by CD133+ surrounded by a relative abundance of CAF (left), compared to CD133- cells (right, Fig 8D). In a third patient tumor sample, the CD133- cells are in close proximity to both  $\alpha$ -SMA+ and  $\alpha$ -SMA- CAF (Fig 8E); however, the CD133+ cells are surrounded by predominately  $\alpha$ -SMA+ CAF. Close-up representative paired CD133- and CD133+ cells from the 11 additional patients are shown in Fig 9. In six of these patient samples, CK20 and CK7 staining were also performed. Three of the 6 colon cancer specimens were CK20+/CK7-, similar to the majority of colon cancers (31), and the other three were double positive for CK20 and CK7 (data not shown). The close proximity of CD133+ cells to CAF support our hypothesis that CD133+ cells better poised to interact in a paracrine fashion to promote tumor progression compared to CD133- cells.

## DISCUSSION

Experimental studies show that the CD133+ cells have a higher tumorigenic potential among the other malignant cells that comprise a solid tumor. Yet, increased cell proliferation, migration, invasion and tumorigenicity of colorectal cancer cells in nude mice cannot be attributable to a direct function of CD133 because siRNA-mediated knockdown of CD133 has demonstrated no significant differences in these measureable functions compared to non-targeted siRNA control cells (17, 18). Although the specific function of CD133 is unknown, the CD133 phenotype is clearly associated with more aggressive tumor characteristics such as chemotherapy resistance (37, 38) and poor clinical outcome (15, 39). Previously, our understanding of the CD133 phenotype has been limited by the lack of a specific model to address the contributions of the other cells in the tumor microenvironment. In this study, we concurrently isolated the carcinoma cells, along with the CAF, and showed by gene microarray analysis that the CD133+ phenotype is characterized by increased co-expression of cell surface receptors to chemokines and growth factors, increased expression of proteases that can break down matrix proteins, and decreased expression of matrix proteins. We have shown that the CD133+ cell is more tumorigenic in NOD-SCID mice (Fig 3C and D), and molecular profiling (Table 2) suggest that the CD133+ cells may have an advantage over CD133- cells that allows them to cooperate with other cells in the stromal microenvironment, such as their companion CAF, to promote tumor growth, invasion, and metastasis. We demonstrate marked overexpression of functional CXCR4 in a population of CD133+ cells compared to the CD133- cells, and show that the paracrine CXCR4/SDF-1

signaling axis contributes to the growth advantage that CD133+ cells have over the CD133- cells.

Zeelenberg and colleagues (40) previously reported CXCR4-deficient colon cancer cells can colonize the lung parenchyma to the same extent as CXCR4+ cells, but only CXCR4+ cells can grow in this metastatic niche. In this primary colorectal cancer, the CD133+/CXCR4+ population is a candidate cell-type that may be likely to become the metastatic cell type, by interacting with CAF and/or other cell types that secrete SDF-1 $\alpha$ . Furthermore, our analysis revealed that CD133+ cells also overexpress other cell surface receptors that mediate proliferation and metastasis, all of which may contribute to the overall aggressive behavior of CD133+ cells in the tumor microenvironment: fibroblast growth factor receptor-2 (FGFR2), macrophage inhibitory factor receptor (CD74), and integrin  $\beta$ 8 (ITG  $\beta$ 8). The companion CAF derived from the primary colon cancer overexpress the gene transcripts for the activating ligands: the FGF family members, macrophage inhibitory factor (MIF), and extracellular matrix protein vitronectin, respectively (Table 2B and C). ITG  $\beta$ 8 exclusively pairs with  $\alpha$ v (ITGAV) and has been shown to promote neurosphere proliferation and survival of *in vitro* neural progenitor cells (41). ITG  $\beta$ 8 binds vitronectin, a matrix protein found only in the stroma of colorectal cancers and not normal colon mucosa (42), implicating a potential role for  $\beta$ 8 in the microenvironment of colon cancer. MIF is a cytokine secreted by immune cells, CAF, and tumor cells upon inflammation and stress, and has been shown to be a non-cognate ligand of the chemokine receptor CXCR4 (43). CD133+ cells also have relatively increased gene transcript expression for proteases (SULF2, TMPRSS2, PRSS3, CTSO, CTSS) and marked decrease expression for ECM proteins (COL1A1, COL1A2, COL3A1, SPARC, FN1, CSPG2) (<http://www.ncbi.nlm.nih.gov/geo>). By breaking down the surrounding ECM components, proteases facilitate the invasion and metastatic spread of tumor cells, as well as release and activate growth and angiogenic factors. Future studies on CD133+ colon cancer and their CAF involving other receptor-ligand pairs will reveal potentially important paracrine signaling systems.

Other investigators have shown that engraftment of human tumors in mice is dependent on the specific mouse strain, which harbor the critical microenvironment necessary for supporting tumor cell growth. Kelly and colleagues (44) demonstrated that while only a few human acute myeloid leukemia (AML) cells can survive in irradiated NOD-SCID mice, a large proportion of murine lymphoid or myeloid malignant cells engrafted into non-irradiated NOD-SCID mice, and these mice developed disseminated disease with very high frequency. Quintana et al. (45) also confirmed that tumorigenesis is very dependent on a permissive microenvironment. They found that human melanoma cells injected into NOD-SCID mice were significantly less tumorigenic (1:46,700 cells engrafted) compared to the same cells injected into the more immunocompromised NOD-SCID-IL2R $\gamma$ <sup>-/-</sup> mice (1:9 cells engrafted), which lack the interleukin-2 $\gamma$  receptor responsible for natural killer cell activity. Recently, Vermulen et al. (46) demonstrated that CAF derived hepatocyte growth factor (HGF) activated c-met on colon cancer stem cells to promote cell growth via  $\beta$ -catenin-dependent transcriptional activation. Together, these recent studies underscore the importance of studying the colon cancer CD133+ cell phenotype in the context of its

relevant microenvironment (e.g., in association with the accompanying CAF). After the establishment of distant metastasis, CD133 expression is downregulated, and is no longer essential for the initiation of tumors in xenografts (47). Shmelkov et al. (47) showed that metastatic CD133+ colorectal cancer cells can propagate into both CD133+ and CD133- cells, and both subpopulations subsequently have the ability to initiate tumorigenesis in NOD-SCID mice, suggesting that the metastatic cancer cells may have acquired alternative ways to sustain tumor growth that does not involve the CD133 cell surface marker. Future studies are needed to address the possibility that CD133 is important for the initiation and progression of primary tumors, but not necessary after the tumor has successfully spread distantly.

Our data support the contention that the pro-tumorigenic potential of the CD133+ cancer cell type is dependent on specific microenvironmental determinants. Each primary colorectal cancer not only has a unique cancer genome, but also has specific reciprocal (paracrine) relationships between the epithelial and stromal components, all of which contribute to the biological behavior of that specific tumor, including the CAF, tumor-associated macrophages (48), other hematopoietic cells, and vascular endothelial cells (49). In this report, we show that 1) CD133+ cells are a heterogeneous cell population and that 2) the co-expression of additional cell surface receptors, for example CXCR4, mediates a critical paracrine signaling axis, indicating that the enhanced tumorigenic properties attributable to CD133 phenotype relies on the subpopulation of CD133+ cells that can interact with its microenvironment. Future studies, particularly *in vivo* tumorigenesis studies, are needed to verify a paracrine signaling loop between CAF and CD133+ colorectal cancers. In the emerging era of “personalized medicine” for the treatment of cancers, it will be important to define patient-specific therapies based on the molecular characteristics of the individual’s tumor, as well as the specific paracrine signaling axes promoted in the cancer microenvironment.

## Supplementary Material

Refer to Web version on PubMed Central for supplementary material.

## ACKNOWLEDGMENTS

**Sources of support:** Dr. Chao is supported by a research career development award 1K08CA12520901A2 and Society of Surgical Oncology Clinical Investigator Award.

We thank Eileen Figueroa, Steve Schuenke, and Karen Martin for their assistance with the preparation of this manuscript, and Sumeet Batra, Kenneth Escobar and Kerry Graves for their technical assistance.

## List of abbreviations

<b>AML</b>	acute myeloid leukemia
<b>CAFs</b>	cancer-associated fibroblasts
<b>CD133-</b>	CD133-negative
<b>CD133+</b>	CD133-positive

<b>ECM</b>	extracellular matrix
<b>FACS</b>	fluorescence-activated cell sorting
<b>H&amp;E</b>	hematoxylin and eosin
<b>HGF</b>	hepatocyte growth factor
<b>IHC</b>	immunohistochemistry
<b>ITG <math>\beta</math>8</b>	integrin $\beta$ 8
<b>PBS</b>	phosphate buffered saline
<b>qPCR</b>	real-time PCR validation
<b>SMA</b>	smooth muscle actin
<b>TUNEL</b>	TdT-mediated dUTP Nick-End Labeling

## REFERENCES

1. Miraglia S, Godfrey W, Yin AH, et al. A novel five-transmembrane hematopoietic stem cell antigen: isolation, characterization, and molecular cloning. *Blood*. 1997; 90:5013–5021. [PubMed: 9389721]
2. Yin AH, Miraglia S, Zanjani ED, et al. AC133, a novel marker for human hematopoietic stem and progenitor cells. *Blood*. 1997; 90:5002–5012. [PubMed: 9389720]
3. Collins AT, Berry PA, Hyde C, Stower MJ, Maitland NJ. Prospective identification of tumorigenic prostate cancer stem cells. *Cancer Res*. 2005; 65:10946–10951. [PubMed: 16322242]
4. Hermann PC, Huber SL, Herrler T, et al. Distinct populations of cancer stem cells determine tumor growth and metastatic activity in human pancreatic cancer. *Cell Stem Cell*. 2007; 1:313–323. [PubMed: 18371365]
5. Ma S, Chan KW, Hu L, et al. Identification and characterization of tumorigenic liver cancer stem/progenitor cells. *Gastroenterology*. 2007; 132:2542–2556. [PubMed: 17570225]
6. Maw MA, Corbeil D, Koch J, et al. A frameshift mutation in prominin (mouse)-like 1 causes human retinal degeneration. *Hum Mol Genet*. 2000; 9:27–34. [PubMed: 10587575]
7. O'Brien CA, Pollett A, Gallinger S, Dick JE. A human colon cancer cell capable of initiating tumour growth in immunodeficient mice. *Nature*. 2007; 445:106–110. [PubMed: 17122772]
8. Ricci-Vitiani L, Lombardi DG, Pilozzi E, et al. Identification and expansion of human colon-cancer-initiating cells. *Nature*. 2007; 445:111–115. [PubMed: 17122771]
9. Richardson GD, Robson CN, Lang SH, Neal DE, Maitland NJ, Collins AT. CD133, a novel marker for human prostatic epithelial stem cells. *J Cell Sci*. 2004; 117:3539–3545. [PubMed: 15226377]
10. Rutella S, Bonanno G, Procoli A, et al. Cells with characteristics of cancer stem/progenitor cells express the CD133 antigen in human endometrial tumors. *Clin Cancer Res*. 2009; 15:4299–4311. [PubMed: 19509143]
11. Singh SK, Clarke ID, Terasaki M, et al. Identification of a cancer stem cell in human brain tumors. *Cancer Res*. 2003; 63:5821–5828. [PubMed: 14522905]
12. Yin S, Li J, Hu C, et al. CD133 positive hepatocellular carcinoma cells possess high capacity for tumorigenicity. *Int J Cancer*. 2007; 120:1444–1450. [PubMed: 17205516]
13. Ieta K, Tanaka F, Haraguchi N, et al. Biological and genetic characteristics of tumor-initiating cells in colon cancer. *Ann Surg Oncol*. 2008; 15:638–648. [PubMed: 17932721]
14. Artells R, Moreno I, Diaz T, et al. Tumour CD133 mRNA expression and clinical outcome in surgically resected colorectal cancer patients. *Eur J Cancer*. 2010; 46:642–649. [PubMed: 20005089]

15. Horst D, Kriegl L, Engel J, Kirchner T, Jung A. CD133 expression is an independent prognostic marker for low survival in colorectal cancer. *Br J Cancer*. 2008; 99:1285–1289. [PubMed: 18781171]
16. Yasuda H, Tanaka K, Saigusa S, et al. Elevated CD133, but not VEGF or EGFR, as a predictive marker of distant recurrence after preoperative chemoradiotherapy in rectal cancer. *Oncol Rep*. 2009; 22:709–717. [PubMed: 19724847]
17. Du L, Wang H, He L, et al. CD44 is of functional importance for colorectal cancer stem cells. *Clin Cancer Res*. 2008; 14:6751–6760. [PubMed: 18980968]
18. Horst D, Scheel SK, Liebmann S, et al. The cancer stem cell marker CD133 has high prognostic impact but unknown functional relevance for the metastasis of human colon cancer. *J Pathol*. 2009; 219:427–434. [PubMed: 19621338]
19. Bhowmick NA, Neilson EG, Moses HL. Stromal fibroblasts in cancer initiation and progression. *Nature*. 2004; 432:332–337. [PubMed: 15549095]
20. Tlsty TD, Coussens LM. Tumor stroma and regulation of cancer development. *Annu Rev Pathol*. 2006; 1:119–150. [PubMed: 18039110]
21. Desmouliere A, Guyot C, Gabbiani G. The stroma reaction myofibroblast: a key player in the control of tumor cell behavior. *Int J Dev Biol*. 2004; 48:509–517. [PubMed: 15349825]
22. Olumi AF, Grossfeld GD, Hayward SW, Carroll PR, Tlsty TD, Cunha GR. Carcinoma-associated fibroblasts direct tumor progression of initiated human prostatic epithelium. *Cancer Res*. 1999; 59:5002–5011. [PubMed: 10519415]
23. Orimo A, Gupta PB, Sgroi DC, et al. Stromal fibroblasts present in invasive human breast carcinomas promote tumor growth and angiogenesis through elevated SDF-1/CXCL12 secretion. *Cell*. 2005; 121:335–348. [PubMed: 15882617]
24. Hwang RF, Moore T, Arumugam T, et al. Cancer-associated stromal fibroblasts promote pancreatic tumor progression. *Cancer Res*. 2008; 68:918–926. [PubMed: 18245495]
25. Teicher BA, Fricker SP. CXCL12 (SDF-1)/CXCR4 pathway in cancer. *Clin Cancer Res*. 2010; 16:2927–2931. [PubMed: 20484021]
26. Chao C, Tallman ML, Ives KL, Townsend CM Jr, Hellmich MR. Gastrointestinal hormone receptors in primary human colorectal carcinomas. *J Surg Res*. 2005; 129:313–321. [PubMed: 16051276]
27. Tsien RY, Harootunian AT. Practical design criteria for a dynamic ratio imaging system. *Cell Calcium*. 1990; 11:93–109. [PubMed: 2354507]
28. Kalluri R, Zeisberg M. Fibroblasts in cancer. *Nat Rev Cancer*. 2006; 6:392–401. [PubMed: 16572188]
29. Bauer N, Fonseca AV, Florek M, et al. New insights into the cell biology of hematopoietic progenitors by studying prominin-1 (CD133). *Cells Tissues Organs*. 2008; 188:127–138. [PubMed: 18160824]
30. Vermeulen L, Todaro M, de Sousa Mello F, et al. Single-cell cloning of colon cancer stem cells reveals a multi-lineage differentiation capacity. *Proc Natl Acad Sci U S A*. 2008; 105:13427–13432. [PubMed: 18765800]
31. Tot T. Cytokeratins 20 and 7 as biomarkers: usefulness in discriminating primary from metastatic adenocarcinoma. *Eur J Cancer*. 2002; 38:758–763. [PubMed: 11937308]
32. Dalerba P, Dylla SJ, Park IK, et al. Phenotypic characterization of human colorectal cancer stem cells. *Proc Natl Acad Sci U S A*. 2007; 104:10158–10163. [PubMed: 17548814]
33. Levin TG, Powell AE, Davies PS, et al. Characterization of the intestinal cancer stem cell marker CD166 in the human and mouse gastrointestinal tract. *Gastroenterology*. 2010; 139:2072–2082. e2075. [PubMed: 20826154]
34. Mori T, Doi R, Koizumi M, et al. CXCR4 antagonist inhibits stromal cell-derived factor 1-induced migration and invasion of human pancreatic cancer. *Mol Cancer Ther*. 2004; 3:29–37. [PubMed: 14749473]
35. Sutton A, Friand V, Brule-Donneger S, et al. Stromal cell-derived factor-1/chemokine (C-X-C motif) ligand 12 stimulates human hepatoma cell growth, migration, and invasion. *Mol Cancer Res*. 2007; 5:21–33. [PubMed: 17259344]

36. Yang WL, Frucht H. Cholinergic receptor up-regulates COX-2 expression and prostaglandin E(2) production in colon cancer cells. *Carcinogenesis*. 2000; 21:1789–1793. [PubMed: 11023534]
37. Dallas NA, Xia L, Fan F, et al. Chemoresistant colorectal cancer cells, the cancer stem cell phenotype, and increased sensitivity to insulin-like growth factor-I receptor inhibition. *Cancer Res*. 2009; 69:1951–1957. [PubMed: 19244128]
38. Todaro M, Perez Alea M, Scopelliti A, Medema JP, Stassi G. IL-4-mediated drug resistance in colon cancer stem cells. *Cell Cycle*. 2008; 7:309–313. [PubMed: 18235245]
39. Takahashi S, Kamiyama T, Tomaru U, et al. Frequency and pattern of expression of the stem cell marker CD133 have strong prognostic effect on the surgical outcome of colorectal cancer patients. *Oncol Rep*. 2010; 24:1201–1212. [PubMed: 20878111]
40. Zeelenberg IS, Ruuls-Van Stalle L, Roos E. The chemokine receptor CXCR4 is required for outgrowth of colon carcinoma micrometastases. *Cancer Res*. 2003; 63:3833–3839. [PubMed: 12839981]
41. Mobley AK, Tchaicha JH, Shin J, Hossain MG, McCarty JH. Beta8 integrin regulates neurogenesis and neurovascular homeostasis in the adult brain. *J Cell Sci*. 2009; 122:1842–1851. [PubMed: 19461074]
42. Tomasini-Johansson BR, Sundberg C, Lindmark G, Gailit JO, Rubin K. Vitronectin in colorectal adenocarcinoma--synthesis by stromal cells in culture. *Exp Cell Res*. 1994; 214:303–312. [PubMed: 7521845]
43. Vera PL, Iczkowski KA, Wang X, Meyer-Siegler KL. Cyclophosphamide-induced cystitis increases bladder CXCR4 expression and CXCR4-macrophage migration inhibitory factor association. *PLoS One*. 2008; 3:e3898. [PubMed: 19066630]
44. Kelly PN, Dakic A, Adams JM, Nutt SL, Strasser A. Tumor growth need not be driven by rare cancer stem cells. *Science*. 2007; 317:337. [PubMed: 17641192]
45. Quintana E, Shackleton M, Sabel MS, Fullen DR, Johnson TM, Morrison SJ. Efficient tumour formation by single human melanoma cells. *Nature*. 2008; 456:593–598. [PubMed: 19052619]
46. Vermeulen L, De Sousa EMF, van der Heijden M, et al. Wnt activity defines colon cancer stem cells and is regulated by the microenvironment. *Nat Cell Biol*. 2010; 12:468–476. [PubMed: 20418870]
47. Shmelkov SV, Butler JM, Hooper AT, et al. CD133 expression is not restricted to stem cells, and both CD133+ and CD133- metastatic colon cancer cells initiate tumors. *J Clin Invest*. 2008; 118:2111–2120. [PubMed: 18497886]
48. Condeelis J, Pollard JW. Macrophages: obligate partners for tumor cell migration, invasion, and metastasis. *Cell*. 2006; 124:263–266. [PubMed: 16439202]
49. Murdoch C, Muthana M, Coffelt SB, Lewis CE. The role of myeloid cells in the promotion of tumour angiogenesis. *Nat Rev Cancer*. 2008; 8:618–631. [PubMed: 18633355]



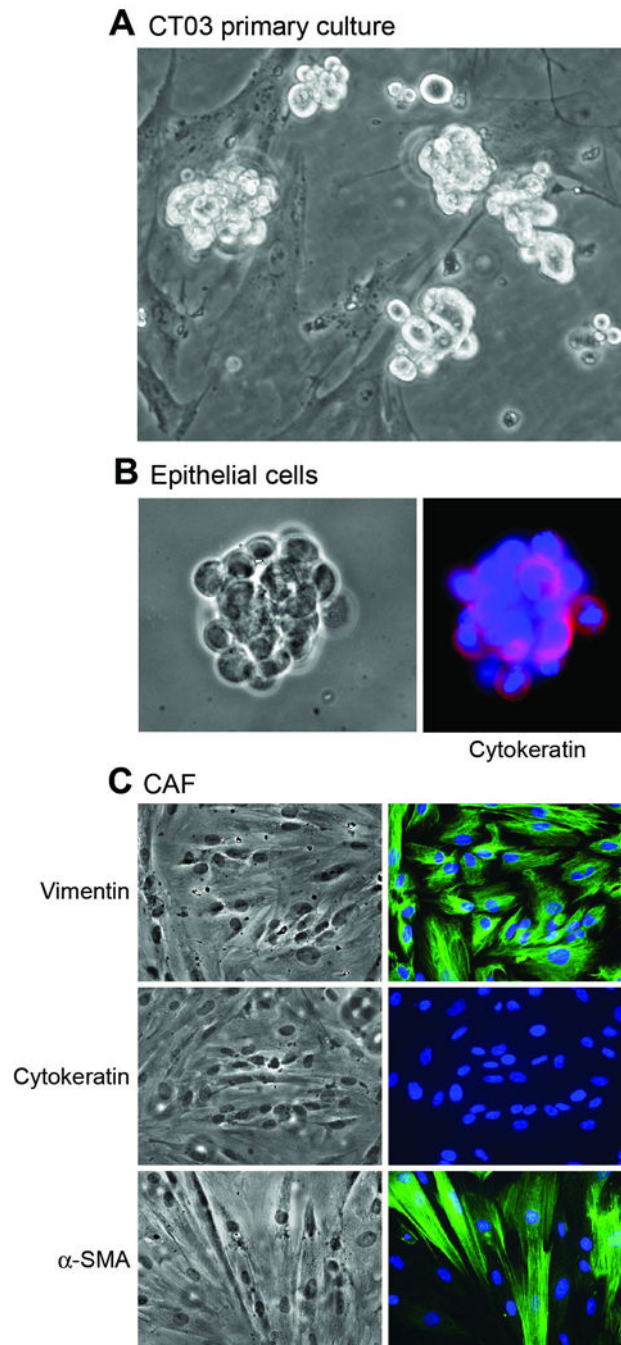


**Figure 1.**

Phase contrast image of characteristic features of primary colon cancer cells and CAF isolated from a patient with Stage II disease maintained. (A) Mixed cell population with two phenotypes in cell culture, consisting of (B), a non-adherent colon cancer cell line that form spheres in culture (phase contrast microscopy) that is cytochrome c-positive (pan- cytochrome c AE1/3), and (C) carcinoma-associated fibroblasts (CAF) that stain for vimentin, but not cytochrome c, with a subpopulation that are  $\alpha$ -SMA-positive. Original Magnification 400X.

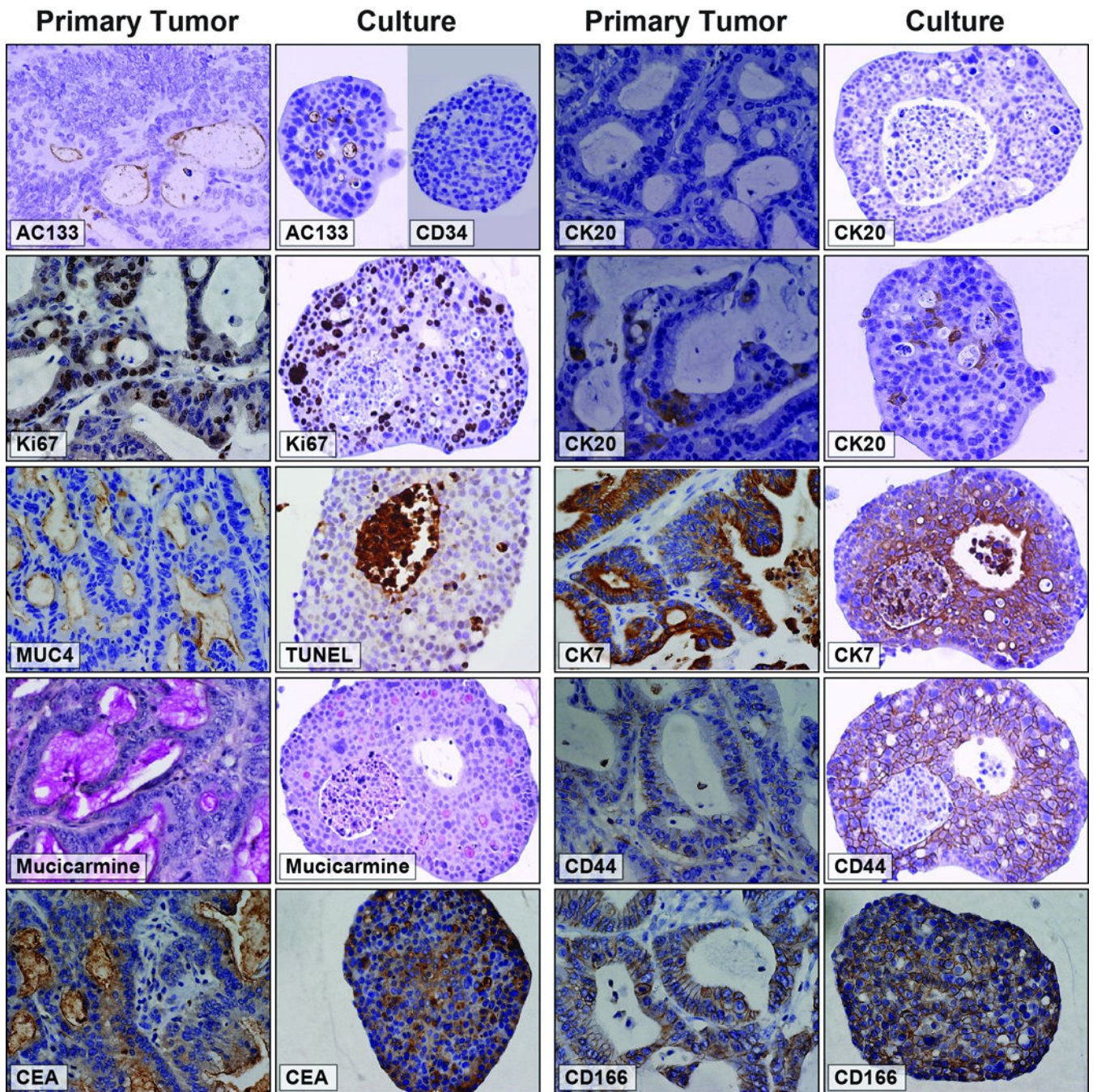


**Figure 2.** Immunohistochemical characterization of the original patient tumor sample (400× original magnification), compared to the colospheres maintained *in vitro* (200× original magnification).

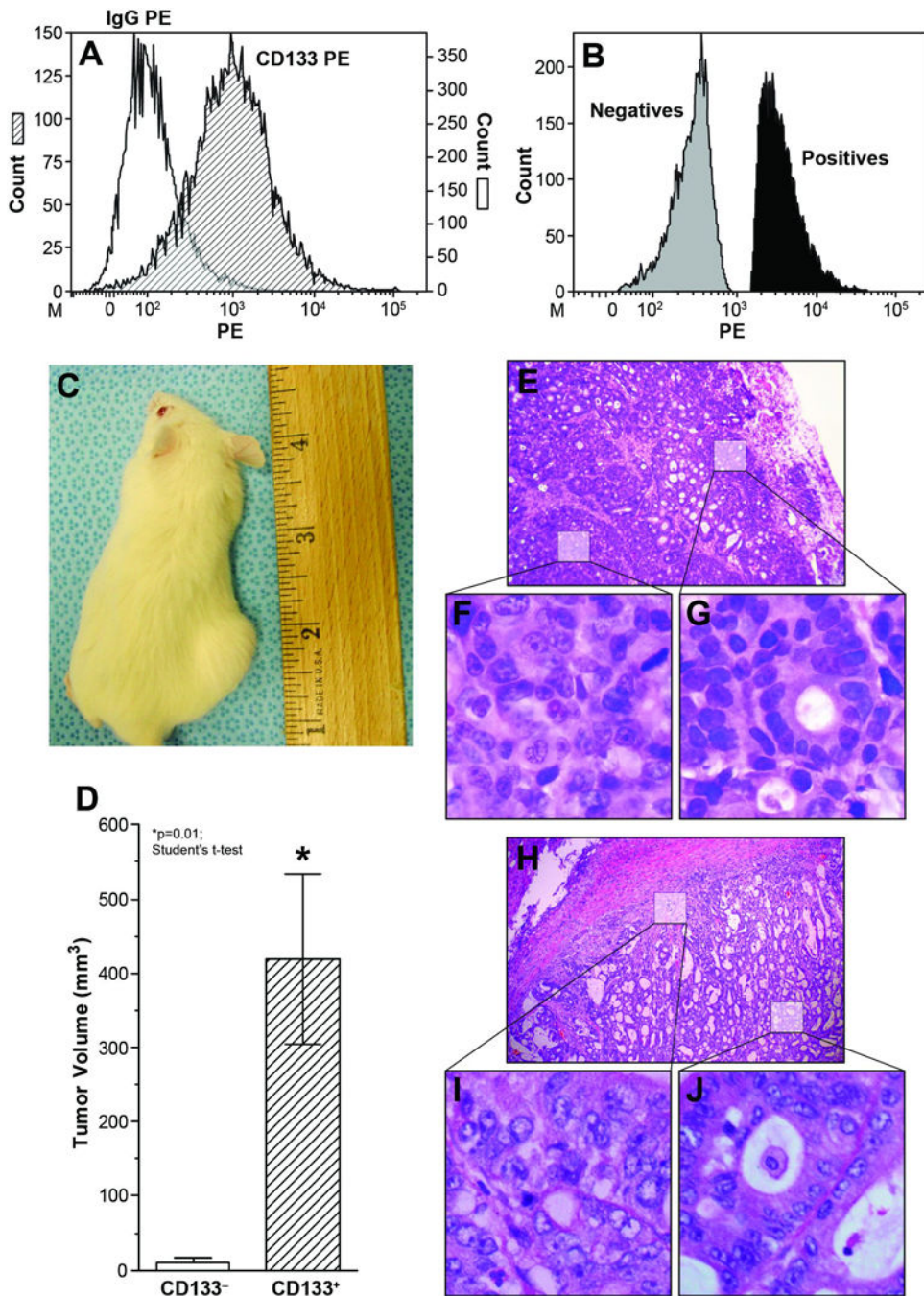


**Figure 3.**

(A) Comparison of fluorescence by colon cancer cells labeled with AC133, an antibody to CD133 conjugated to R-phycoerythrin (PE) and isotype-matched IgG controls labeled with PE (Miltenyi Biotec; Auburn, CA). (B) Fractions colon cancer cells with high expression levels of CD133 (positives) and relatively low expression levels (negatives) collected by fluorescence-activated cell sorting (C) CD133<sup>+</sup> and CD133<sup>-</sup> cells were serially diluted, resuspended in Matrigel, and injected subcutaneously in NOD-SCID mice to assay for tumorigenic potential; representative mouse injected with CD133<sup>+</sup> cells at sacrifice shown.

(D) Summary of tumor volumes measured at 6 weeks comparing CD133- vs. CD133+ tumors. (E) Representative hematoxylin and eosin stain (H&E) of the tumor xenograft (40×). (F, G) Inset from xenograft tumor demonstrates a moderately differentiated tumor and well-differentiated tumor forming glandular structures (400×), respectively. (H) Representative H&E of the tumor from the patient's tumor block (40×). (I, J) H&E (400X) from patient's original tumor block showing similar cellular features from the mouse xenograft, moderately and well-differentiated features.

Author Manuscript

Author Manuscript

Author Manuscript

Author Manuscript

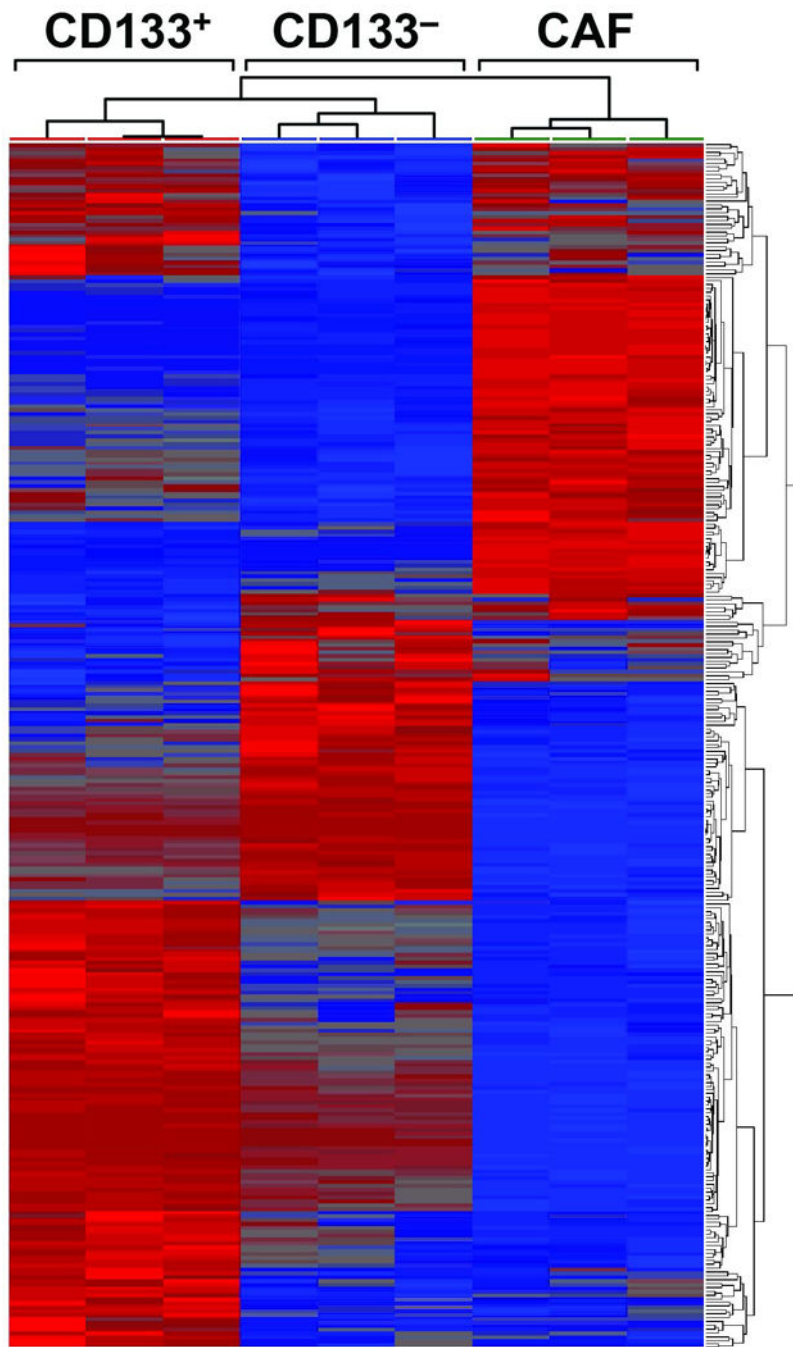


**Figure 4.** Heat Map Comparing CD133+, CD133- colon cancer cells with the accompanying CAF cells. Unsupervised hierarchical clustering comparing the CD133+, CD133-, and CAF cells.

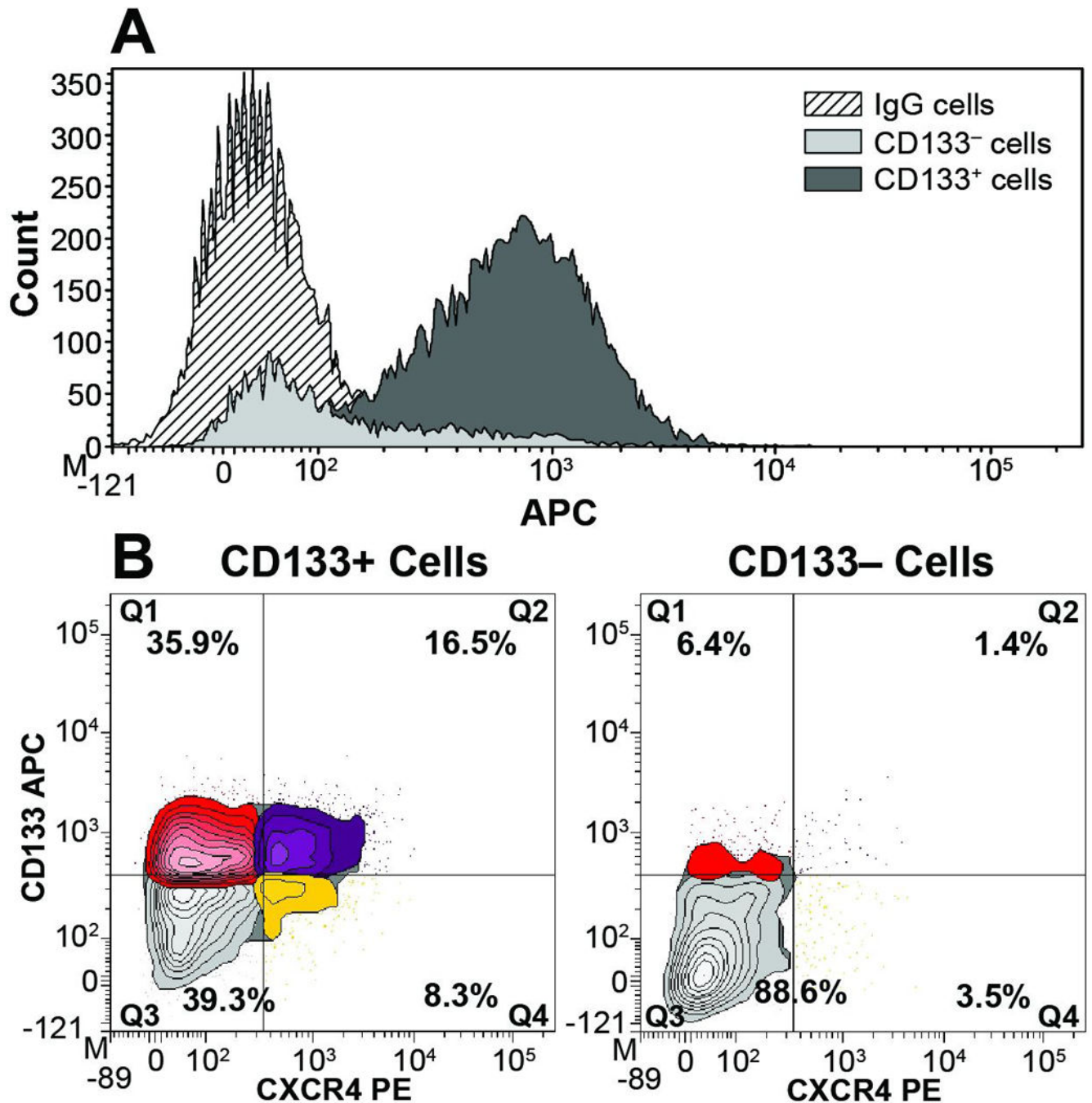


**Figure 5.**

Colospheres, enriched for CD133<sup>+</sup> or relative lack of CD133 (CD133<sup>-</sup>), sorted by flow cytometry, were maintained in culture for up to 8 weeks. (A) Overlay of histograms (from left to right) comparing fluorescence of CD133<sup>+</sup> cells labeled with IgG-APC (negative control), AC133-labelled CD133<sup>-</sup> cells, and AC133-labelled CD133<sup>+</sup> (enriched) cells. (B) After 8 weeks, the enriched cells each maintained their respective CD133 phenotype. Co-expression of cell surface CD133 and CXCR4 in CD133<sup>+</sup> cells and CD133<sup>-</sup> cells.

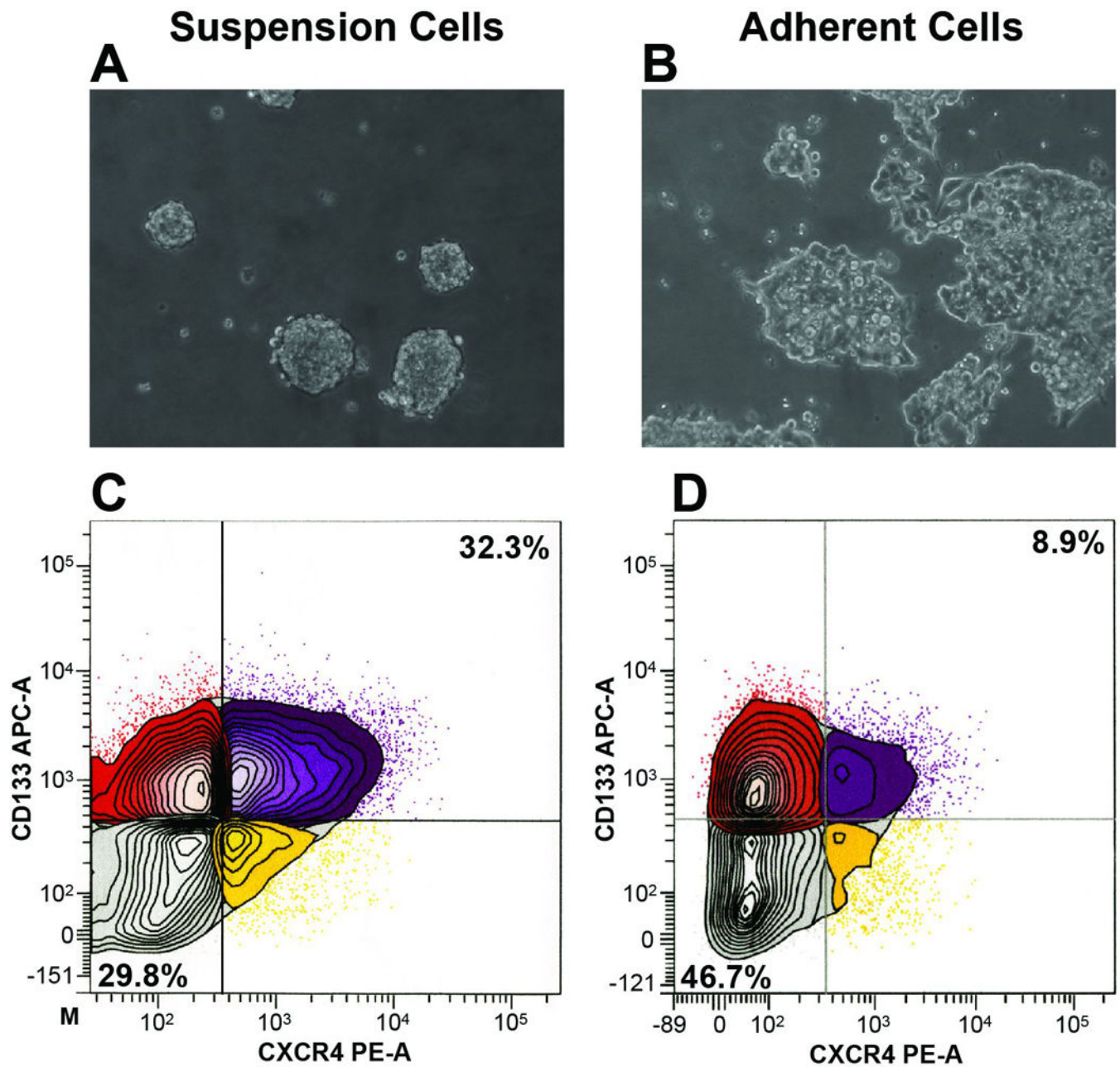


**Figure 6.** Effects of growth conditions (suspension vs. attached) on co-expression of CD133 and CXCR4. (A) Photomicrograph (400×) of colon cancer cells grown in suspension culture (low adhesion flasks). The cells maintain anchorage-independence growth after 9 days. (B) Photomicrograph (400×) of same cells grown in standard tissue culture flasks. After 9–14 days, the cells adhere to the bottom of the flask and exhibit a spread phenotype, consistent with anchorage dependence. (C) FACS analysis demonstrating that when grown in suspension culture, 32% of the cells are double-positive for cell surface CD133 and CXCR4, and that 30% of cells are double-negative for both receptors. (D) When the cells are allowed

to adhere and spread, the double-positive cells decrease to 8.9%, while the double-negative cells increase to 46.7%.

Author Manuscript

Author Manuscript

Author Manuscript

Author Manuscript



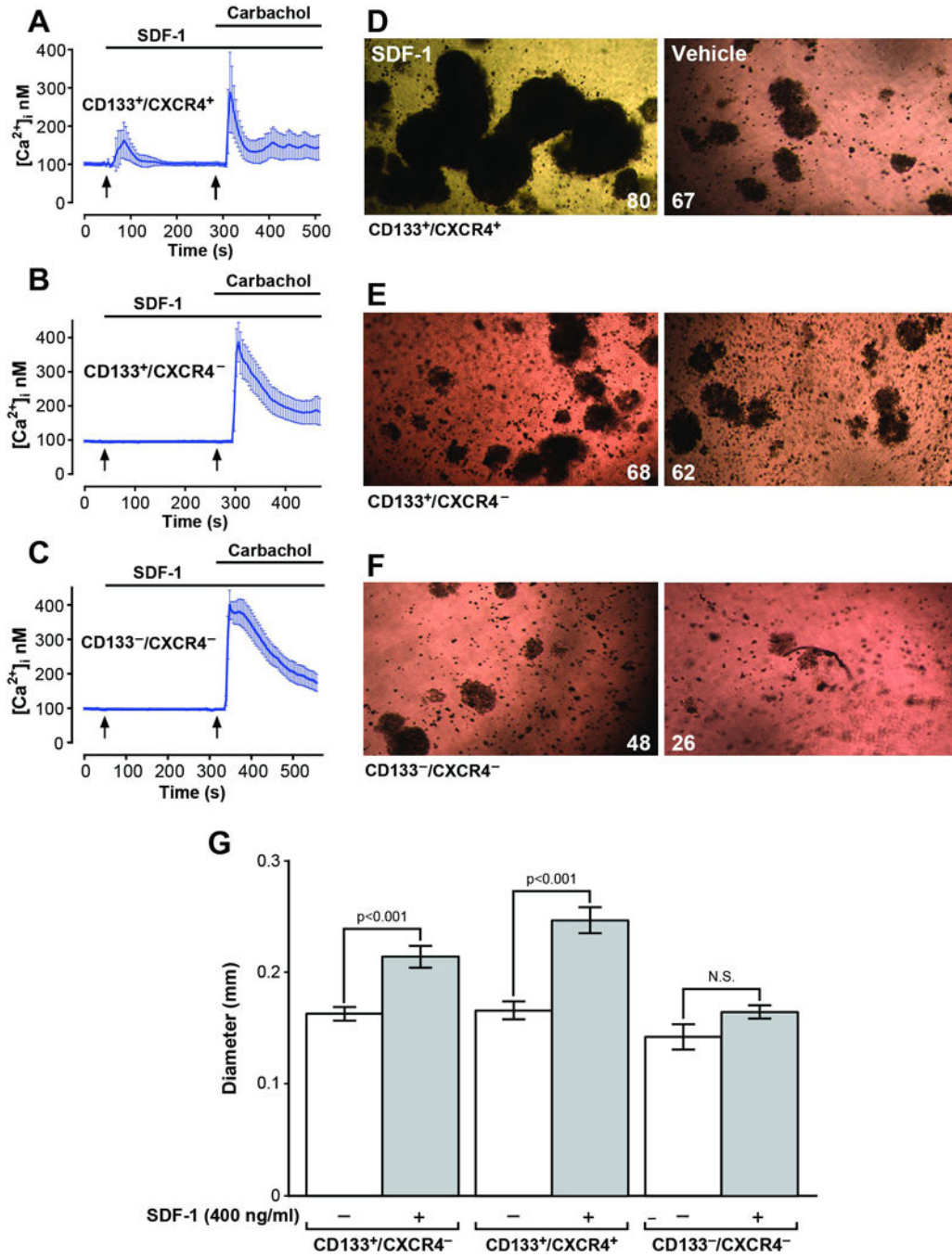


**Figure 7.** Characterization of CD133<sup>+</sup>/CXCR4<sup>+</sup> cells. (A) CD133<sup>+</sup>/CXCR4<sup>+</sup> cells exhibits an increase in intracellular calcium in response to 400 ng/ml of SDF-1 (CXCL12). Subsequent treatment with 10 μM carbachol to insures that the cells were loaded with Fura-2. (B) CD133<sup>+</sup>/CXCR4<sup>-</sup> cells do not respond to SDF-1; however, these cells do have muscarinic receptors, as verified by their calcium response to carbachol, indicating that the calcium indicator dye Fura-2 was loaded in the cells. (C) CD133<sup>-</sup>/CXCR4<sup>-</sup> cells fail to increase intracellular calcium with SDF-1, but does respond to carbachol. (D, E, F) Effects of cell

growth in Matrigel in the presence of SDF-1 (400 ng/ml) or vehicle (0.2% BSA). The average number of cell colonies per well are denoted by the number in the corner of the photo. Photomicrographs (original magnification, 400X) of representative areas of CD133+/CXCR4- (D), CD133+/CXCR4+ (E), CD133-/CXCR4- (F) cell colonies are shown. (G) Bar graph depicting average diameter of the cell colonies, corresponding to figures shown in D, E, F.

Author Manuscript

Author Manuscript

Author Manuscript

Author Manuscript

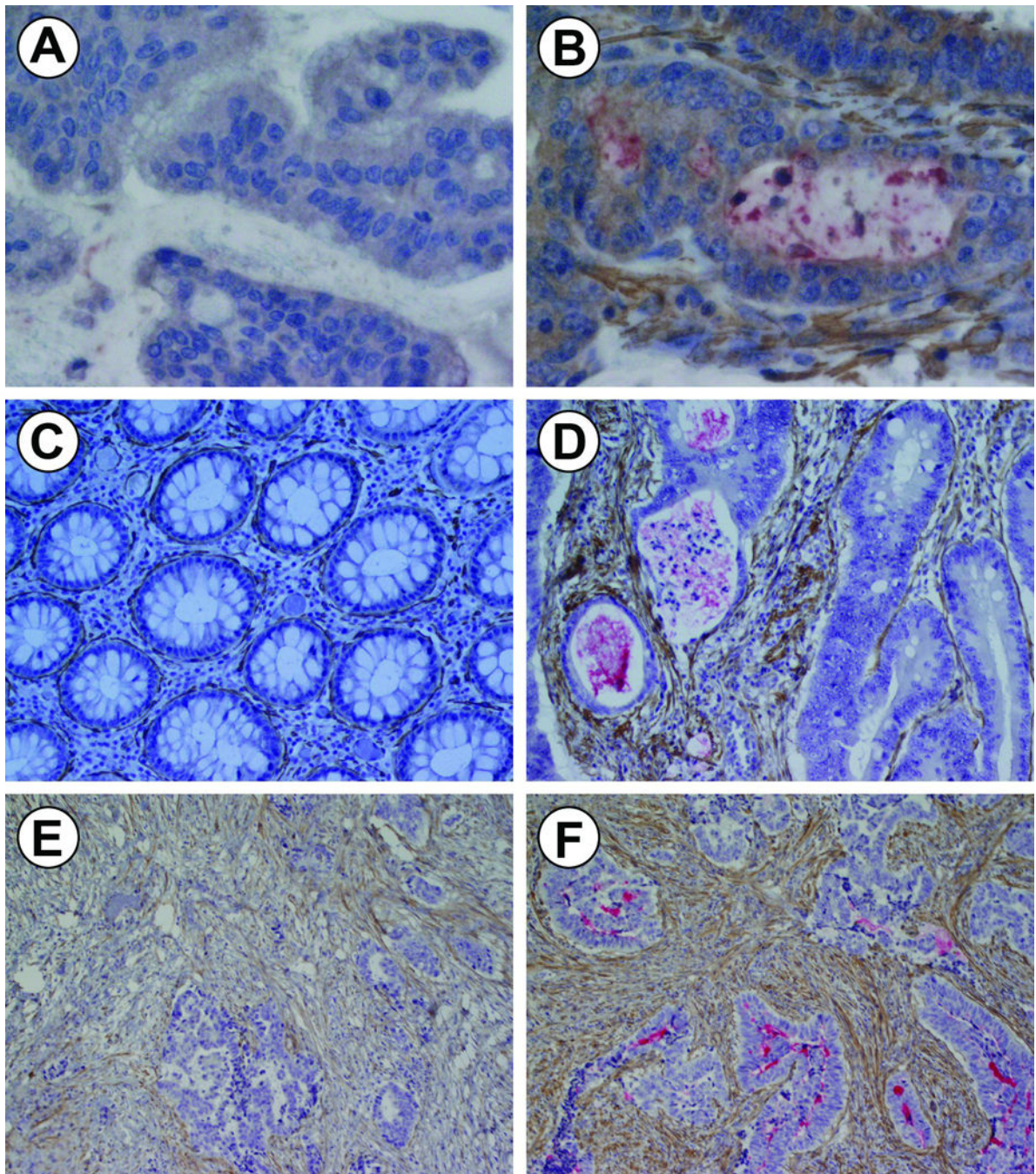


**Figure 8.**

Co-staining of CD133 and  $\alpha$ -SMA showing the spatial relationship between CD133+ cells and CAF, respectively. (A, B) Immunohistochemical characterization of the original patient tumor sample (600 $\times$ , original magnification) of a representative area with (A) CD133 $-$  colon cancer cells and paucity of CAF and (B) CD133+ colon cancer cells (red stain) surrounded by relative abundance of CAF (brown stain). (C, D) Representative area from another patient in area of (C) normal colonic villi surrounded by  $\alpha$ -SMA-positive (brown stain) and (D) malignant tumor with CD133+ (red) and CD133 $-$  cells, 200 $\times$ . (E, F) Colon

cancer from third patient in areas with (E) CD133– colon cancer cells and (F) CD133+ colon cancer cells, 100×.

Author Manuscript

Author Manuscript

Author Manuscript

Author Manuscript

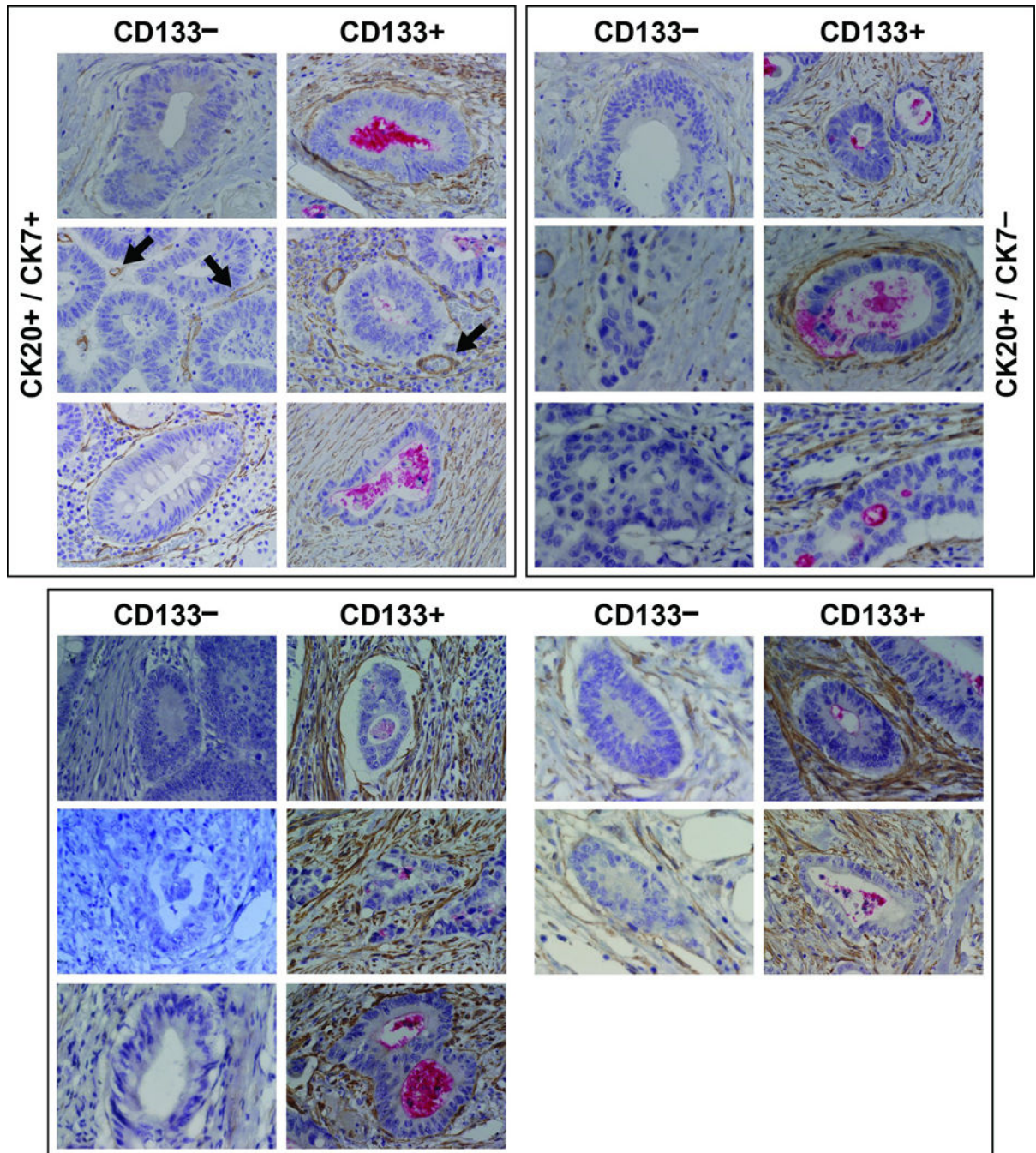


**Figure 9.**

Paired samples of CD133- and CD133+ colon cancer cells from 11 colon cancers. The slides are co-stained for CD133 (red, apical) colon cancer cells and  $\alpha$ -SMA (400 $\times$  and 600 $\times$ ). The arrow demonstrates  $\alpha$ -SMA immunopositivity in the walls of small blood vessels (internal positive control).

**TABLE 1**

Significant Genes Identified by Gene Array Validated by Quantitative Real-Time PCR

Gene Symbol	p-value	Gene Array Fold change	RT-PCR Fold Change
IGFBP3	7.56E-06	1.77362	1.2545
PLECKHB1	1.01E-05	3.22459	1.1764
CP	1.47E-05	2.86229	0.8721
SULF2	7.45E-05	2.20567	1.4212
IFIH1	0.000106	1.36982	0.285
PROM1	0.000168	9.36934	1.774
CEACAM5	0.000305	1.37876	0.1536
FZD2	0.000635	1.39114	0.3026
ALDH1A3	0.00088	2.33778	1.2188
SMAD7	0.001114	1.34044	0.4519
PTPRN2	0.001715	2.32938	0.7781
RRM2B	0.002429	1.20816	0.4979
RARRES1	0.002608	2.59494	1.2729
MUC4	0.002968	1.79323	2.9041
CTSS	0.003889	1.6457	1.2689
PRKAR2B	0.004508	2.239	0.6976
ITGB8	0.006254	2.18013	2.1667
PPIC	0.012036	1.24324	0.4395
UBD	0.012722	2.24373	1.1454
CXCR4	0.014884	4.0673	1.3265
TNFAIP2	0.017107	1.327	1.2429
FGFR2	0.017493	1.21569	1.3451
PLCG2	0.020757	1.16869	0.9214
MUC1	0.021106	1.38278	0.6375
SCD5	0.024365	1.72136	0.3941
CD74	0.038686	3.12507	1.3607
MS12	0.040851	1.18797	0.1003

Statistical significance demonstrated at p-value 0.05

Author Manuscript

Author Manuscript

Author Manuscript

Author Manuscript

TABLE 2

Comparison of Reciprocal Relationships between CAF and CD133+ or CD133- Colon Cancer Cells

<b>A. CD133+ vs. CD133- cells</b>			
<b>RECEPTOR (Gene Symbol)</b>		<b>p-value</b>	<b>Fold Change</b>
CXCR4	chemokine (C-X-C motif) receptor 4	0.02*	4.07
CD74	CD74 molecule, major histocompatibility complex, class II invariant chain	0.04*	3.12
ITGB8	integrin, beta 8	0.01*	2.18
FGFR2	Fibroblast growth factor 2	0.03*	1.21
<b>LIGAND</b>			
CXCL12	chemokine (C-X-C motif) ligand 12 (stromal cell-derived factor 1)	0.89	1.02
MIF	macrophage migration inhibitory factor (glycosylation-inhibiting factor)	0.88	1.01
VTN	vitronectin	0.82	-1.04
FGF ligands 1,2,7,5,13,	fibroblast growth factor ligands	N.S.	

<b>B. CAF vs. CD133+ or CD133- cells</b>			
<b>LIGAND</b>		<b>CAF vs CD133+</b>	<b>CAF vs CD133+</b>
		<b>p-value</b>	<b>Fold change</b>
		<b>CAF vs CD133-</b>	<b>CAF vs CD133-</b>
		<b>p-value</b>	<b>Fold change</b>
CXCL12	chemokine (C-X-C motif) ligand 12 (stromal cell-derived factor 1)	0.0003*	3.73
		0.0002*	3.8
MIF	macrophage migration inhibitory factor (glycosylation-inhibiting factor)	3.71E-05*	1.87
		4.01E-5*	1.85
VTN	vitronectin	1.54E-05*	7.29
		1.72E-05*	7.03
FGF2	fibroblast growth factor 2 (basic)	1.49E-09*	28.32
		1.48E-09*	28.51
FGF7	fibroblast growth factor 7 (keratinocyte growth factor)	3.52E-07*	15.35
		3.52E-07*	15.36
FGF13	fibroblast growth factor 13	3.26E-07*	8.10
		5.22E-07*	7.9
FGF5	fibroblast growth factor 5	2.83E-05*	2.57
		3.50E-05*	2.48

<b>B. CAF vs. CD133+ or CD133- cells</b>			
<b>LIGAND</b>		<b>CAF vs CD133+</b>	<b>CAF vs CD133+</b>
		<b>p-value</b>	<b>Fold change</b>
		<b>CAF vs CD133-</b>	<b>CAF vs CD133-</b>
		<b>p-value</b>	<b>Fold change</b>
FGF1	fibroblast growth factor 1	7.48E-05*	2.12
		3.53E-05*	2.35
<b>C. CD133+ or CD133- Cells vs.CAF</b>			
<b>RECEPTOR (GENE SYMBOL)</b>		<b>CD133+ vs. CAF</b>	<b>CD133+ vs. CAF</b>
		<b>p-value</b>	<b>Fold change</b>
		<b>CD133- vs. CAF</b>	<b>CD133- vs. CAF</b>
		<b>p-value</b>	<b>Fold change</b>
CXCR4	chemokine (C-X-C motif) receptor 4	0.007*	5.26
		0.56	1.29
CD74	CD74 molecule, major histocompatibility complex, class II invariant chain	0.03*	3.32
		0.89	1.06
ITGB8	integrin, beta 8	0.009*	2.04
		0.73	-1.07
FGFR2	Fibroblast growth factor 2	0.005*	1.48
		0.015*	1.22

\* Statistical significance demonstrated at p-value 0.05

Author Manuscript

Author Manuscript

Author Manuscript

Author Manuscript